CHAPTER 2

CHANGES IN SOLIDIFICATION MODE, AND THE MEASUREMENT OF COOLING RATES FOLLOWING SOLIDIFICATION DURING ARC WELDING

2.1 INTRODUCTION

The solidification process in a weld pool has been shown to have a considerable influence upon the properties of the resultant weld. It influences the development of microstructure (Edvardsson *et al.*, 1976), and determines the distribution of alloying elements, and hence the homogeneity of the weld. Previous work on the cooling behaviour of welds (Garland and Kirkwood, 1974; Svensson *et al.*, 1986) has tended to concentrate on the measurement and prediction of cooling rates for the temperature range 800-500°C, because these are important in determining the mechanism of austenite decomposition in the weld. This work, however, is concerned with cooling conditions and solidification processes at, and near, the melting temperature. The microsegregation that occurs during solidification is closely related to the size and morphology of the solidifying phase, the crystal structure of which in turn is dependent upon the cooling rate. For example, it is known that with fast cooling rates, low carbon steels may solidify directly as austenite, when δ-ferrite would be expected for cooling conditions closer to equilibrium (Edvardsson *et al.*, 1976), since substitutional atom diffusion is slower in austenite, solidification with non-equilibrium austenite as the primary phase would profoundly influence the homogeneity of the weld deposit.

It would, therefore, be of great value to relate the primary solidification structure to the solidification parameters. Also, although a few pilot studies have been conducted (Kohno and Jones, 1978; Barlow, 1982) almost no quantitative data have been published giving information about the cooling rates at temperatures near the freezing temperature. However, work on the measurement of the thermal cycle experienced in the heat-affected zone (HAZ) during manual-metal-arc (MMA) welding (Baker, 1976) indicate cooling rates in MMA welding to be particularly fast relative to other welding processes.

The aim of this investigation was to develop, and utilize, a method of measuring

the rate of cooling at the solidification temperature encountered in the welding of low-alloy steels.

2.2 PRIMARY SOLIDIFICATION STRUCTURES

Although, solidification will not occur as austenite in the binary Fe-C system for an alloy containing less than 0.53 wt%C at equilibrium (see Figure 4.1), fast cooling rates can cause the primary solidification mode to be austenitic when ferritic solidification would normally be expected (Räsänen and Tenkula, 1972). In order to demonstrate that this could happen at relatively low carbon concentrations as a consequence of the fast cooling rates encountered in arc welding, two bead-on-plate welds were manufactured using specially-produced high-carbon electrodes.

For the first weld (Weld A), three parallel runs of an electrode with a nominal all-weld deposit composition of Fe-0.31C-1.46Mn-0.79Si wt% (Electrode A) were deposited onto a 20mm thick plate of (Swedish standard) SK1311 steel of nominal composition Fe-0.12C-0.55Mn-0.25Si wt%. A top bead was then deposited onto the buttered plate. The welding conditions were 120A/23V (D.C. +ve), and the welding speed was approximately 4mm/s. The second weld (Weld B) was fabricated under the same conditions, except that a consumable stick electrode of nominal deposit composition Fe-0.42C-1.56Mn-1.03Si wt% (Electrode B) was used. In this case, since the carbon content was particularly high, an additional layer, *i.e.* three runs, of buttering were applied to minimize dilution from the base plate, so that the carbon distribution in the top bead was homogeneous.

The compositions of the electrodes used, and the resultant welds are given in Tables 2.1 and 2.2 respectively.

Electrode	Composition/wt%					
	C	Mn	Si	Cr	P	S
A	0.31	1.46	0.79	0.03	0.11	0.066
B	0.42	1.56	1.03	0.03	0.11	0.066

Table 2.1: Welding rod deposit compositions

Weld	Composition/wt%					
	C	Mn	Si	Cr	P	S
A	0.19	1.40	0.69	0.04	0.012	0.007
B	0.31	1.38	0.92	0.02	0.014	0.011

Table 2.2: Welds 2.1 and 2.2: compositions of top beads

Figures 2.1a and b show the microstructures of Welds A and B. Weld A solidified as δ-ferrite, and subsequently transformed to austenite. The micrograph shows the weld metal microstructure adjacent to the fusion boundary; large austenite grains, whose size is comparable to those of the base metal from which the primary microstructure grew epitaxially, can be seen, delineated by thin regions of discontinuous allotriomorphic ferrite. The location of the prior δ cell boundaries may be seen underlying the prior austenite microstructure, indirectly revealed by solute sensitive etching. It should be noted that this micrograph does not imply that the original δ columnar grains were not larger than the austenite grains, since each δ grain will have comprised many cells. It may be observed that the white cell boundaries do not stop at the prior austenite grain boundaries, meaning that the low carbon weld must have solidified as ferrite.

In Weld B, the solidification substructure does stop at the grain boundaries, indicating direct solidification as austenite. The strong contrast between individual cells is a consequence of the heavy microstructural segregation that is characteristic of an austenitic solidification process (Fredriksson and Stjerndahl, 1976). This behaviour is discussed in greater detail in Chapter 4. The almost complete absence of allotriomorphic ferrite, suppressed by the relatively high alloy content of the weld, should also be noted. The broad horizontal bands in the micrograph are due to solute banding, and correspond to periodic regions of solute enrichment or depletion. They occur as a natural consequence of fluctuations in the power of the arc causing periodic retardations in the advance of the weld pool interface (Davies and Garland, 1975).

In both micrographs, the primary phase is characterised by straight columnar grains, since they grew into a liquid phase, whereas the prior austenite grain

Figures 2.1a and b (overleaf): Microstructure of (a) Weld A, and (b) Weld B, showing solidification as primary ferrite and primary austenite respectively.
Etchants: (a) 2% nitamyl followed by Klemm I tint etch; (b) 2% nital.

a)

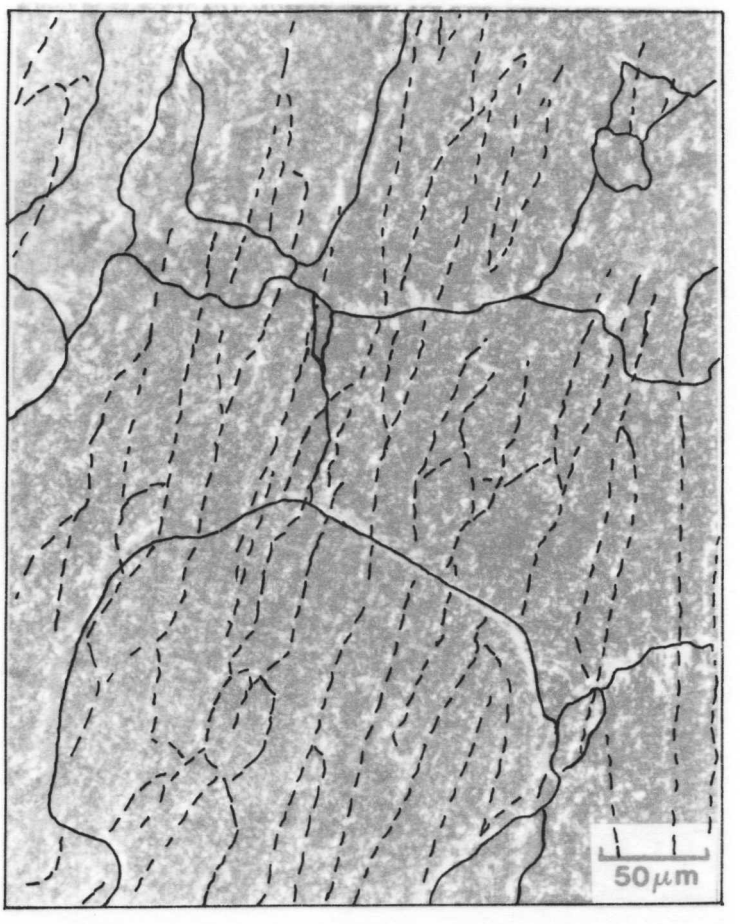

b)

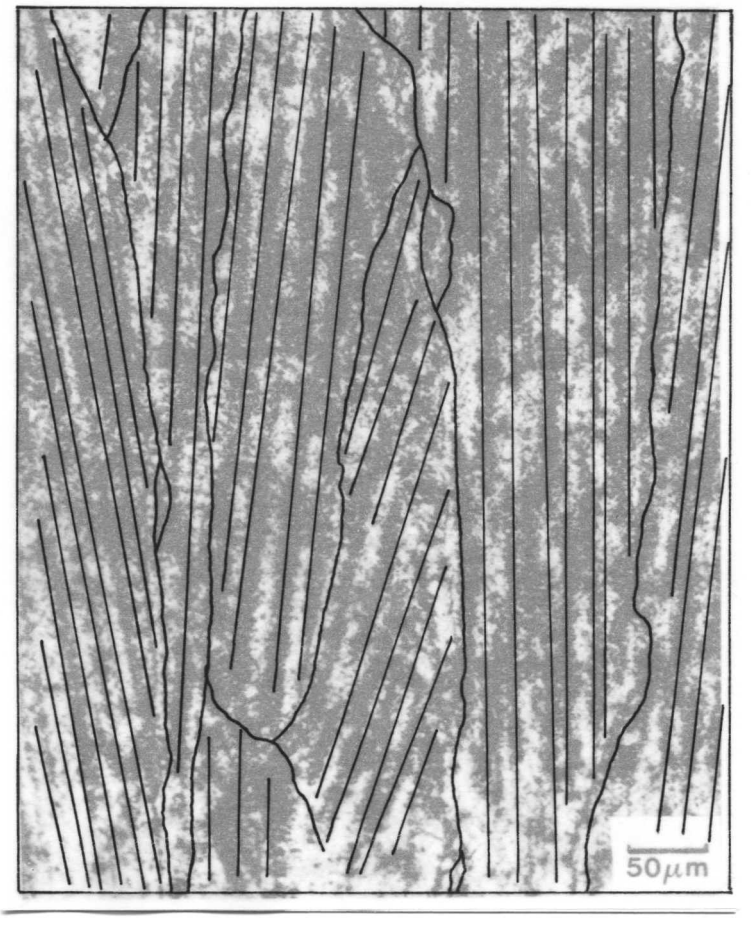

boundaries in Weld A (Figure 2.1a), which are the product of a solid state phase transformation, are irregular.

In summary, therefore, these results demonstrated that for the cooling rates typically found in manual-metal-arc welds, a 0.19 wt% C weld would solidify as ferrite, whereas a 0.31 wt% C weld would solidify as primary austenite. However, it was not known what cooling rates that the welds examined had actually experienced during solidification. It would be interesting to know this, since this would indicate how far the solidification process had been from equilibrium. Jernkontoret (1977) have reported that weld cooling rates vary during solidification between about 20 and 200°C. More accurate information than this, however, was not available, and this led to an enquiry as to how great the physical cooling rates actually were during welding. This is described in the next section.

2.3 EXPERIMENTAL METHOD

Following on from the above work, it was decided to attempt to measure the cooling rates that arise in the fusion zone during arc welding. Temperature measurement was to be carried out using a Pt/Pt-Rh thermocouple, protected by a cylindrical concrete shell. A number of attempts were made to see if pre-insertion of the electrode into the side of the weld would provide a suitable method for recording the temperature. Such a technique has been used in the past for recording the thermal cycles experienced in the HAZ during welding (Barlow, 1982). Unfortunately the high peak temperature encountered in arc welding ensured that the end of the thermocouple was destroyed in each case, (Figs. 2.2(a)-(d)), and the peak temperatures recorded were no more than ~1400°C, indicating that the new tip of the thermocouple was located within the HAZ. It was concluded that preposition-

---

Figures 2.2(a)-(d)) (overleaf): Cross-sections through welds containing sideways pre-inserted thermocouples mounted in bakelite. (Key to schematic diagrams: B = bakelite; BP = base-plate; T = thermocouple; W = weld metal). The micrographs show four single-pass bead-in-groove welds. In each case, a thermocouple has been drilled through the base-plate (on the right of the micrograph) to reach through to the weld. The thermocouples are observed to have received extensive damage as a consequence of the extremely high temperature of the welding arc. Remaining pieces of the thermocouples are arrowed. Etchant: swab-etched in aqueous $NH_4S_2O_3$.

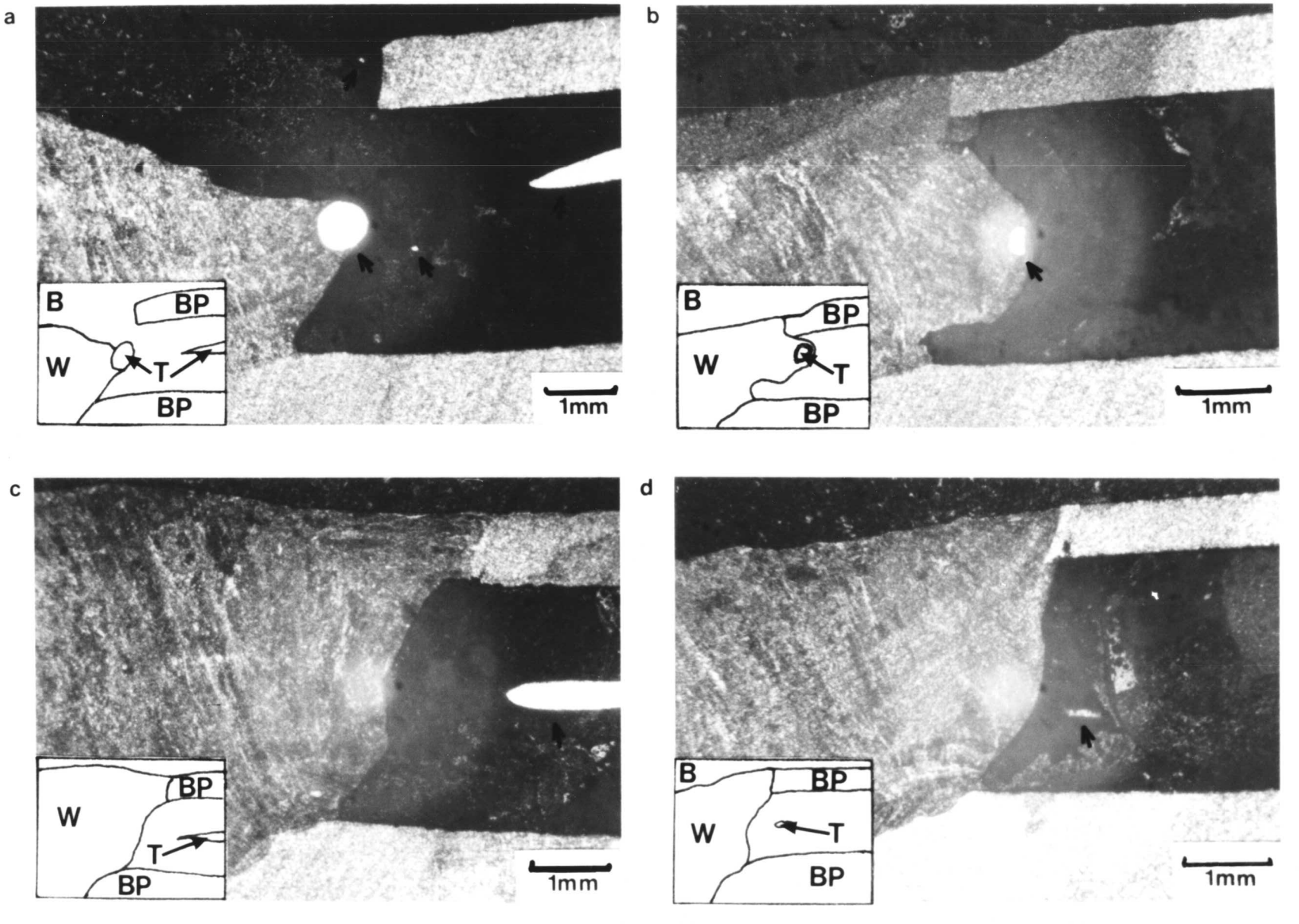
a
B
BP
W
T
BP
1mm
b
B
BP
W
T
BP
1mm
c
W
BP
T
BP
1mm
d
B
BP
W
T
BP
1mm

ing of the thermocouple was unsuitable, although, this does not mean that such a technique could not ultimately be workable as a method for recording cooling rates in the fusion zone; however, harpooning into the weld pool, in which the thermocouple is inserted into the weld pool *after* the welding electrode has passed, seemed to be the best alternative.

A U-shaped groove of radius 5mm was machined onto 12mm thick SK1311 steel plate of nominal composition Fe-0.12C-0.55Mn-0.25Si wt%. OK 48,00 consumable electrode was deposited along this groove. On four occasions, a thermocouple was harpooned into the weld, and the change in temperature was recorded. The current and voltage used during welding were 180A and 22V respectively. Since welding can become very difficult if the current and voltage are changed, different cooling rates were achieved by manipulating the welding speed, v, and the initial temperature of the base plate, T_o. Welding speeds and preheat temperatures for the four welds fabricated (designated Welds 2.1-2.4) are shown in Table 2.3.

Weld ID.	v/mm/s	T_o/C
2.1	2.3	22
2.2	1.4	22
2.3	1.4	610
2.4	1.4	600

Table 2.3: Welding conditions for the cooling curve measurements.

A chart recorder was connected to the thermocouple to produce a permanent record of the change of temperature with time during welding.

One of the disadvantages of harpooning is that the exact position of the thermocouple in the centre of the weld cannot always be guaranteed (Kohno and Jones, 1978). However, Figures 2.3(a)-(d) show that the thermocouples were fairly centrally placed in the weld.

Figures 2.3(a)-(d)) (overleaf): The micrographs show four single-pass welds in cross-section mounted in bakelite. (Key to schematic diagrams: B = bakelite; T = thermocouple; W = weld metal). A thermocouple within a concrete shell was harpooned into each weld immediately after welding. Note that the thermocouples

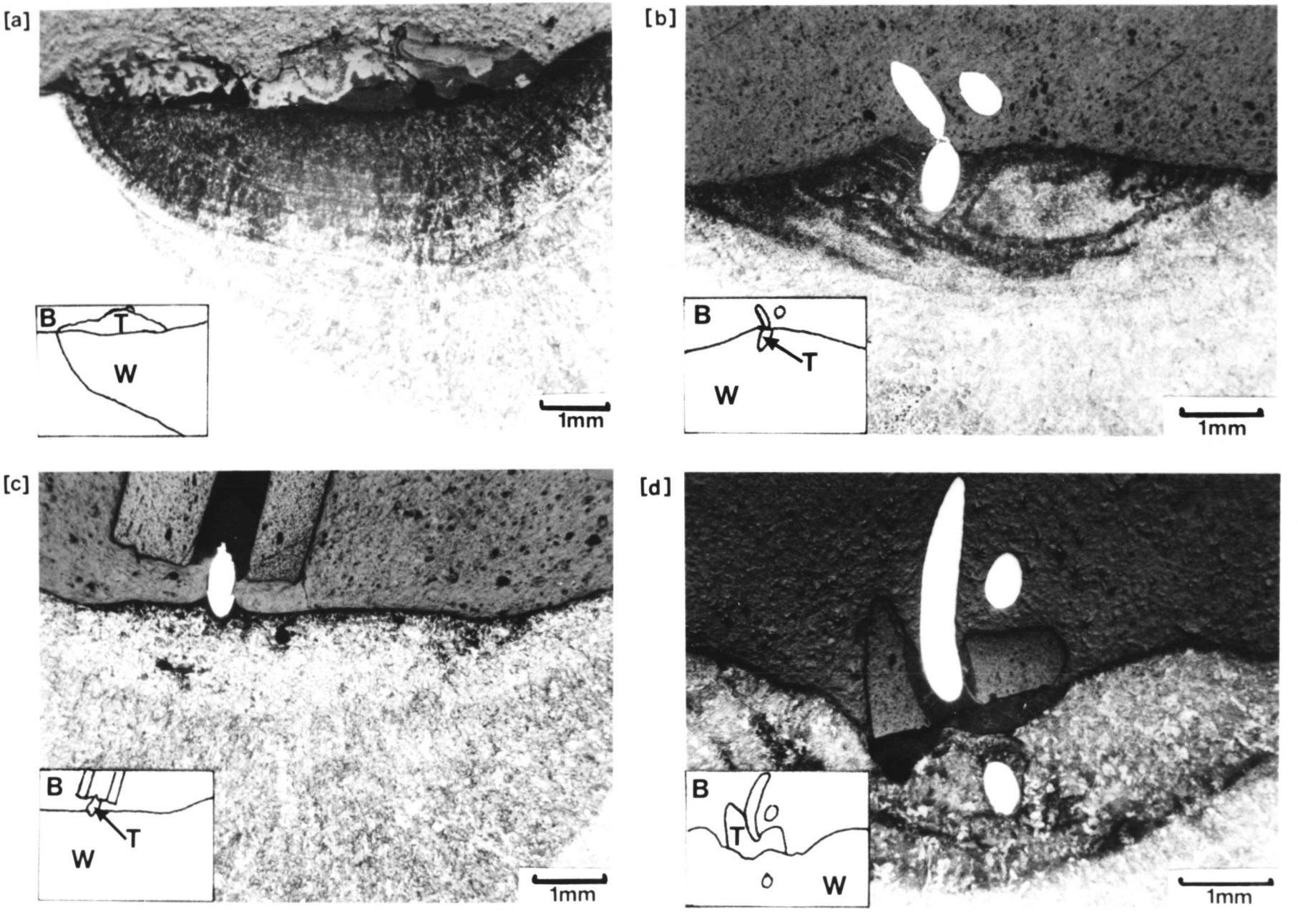
[a]
B
T
W
1mm
[b]
B
T
W
1mm
[c]
B
T
W
1mm
[d]
B
T
W
1mm

When the thermocouple is harpooned into the weld pool during welding, an increase in temperature is recorded. The thermocouple almost immediately becomes fixed to the underlying metal, and as the weld pool moves relative to the thermocouple, so the temperature decreases. With harpooning, the thermocouple does not experience the full severity of the arc, and accordingly, the tip of the thermocouple should not have been destroyed. Yet, in all four cases the recorded temperature did not exceed 1510°C. This is because a finite amount of time is required for the heat to overcome the thermal inertia of the thermocouple device, and to allow the heat to penetrate through the concrete shell to the thermocouple, during which time substantial cooling occurs in the rapidly-cooling weld deposit. However, the central positioning of the thermocouples indicated that the cooling curves that were recorded did represent the absolute cooling rates of the welds.

Figure 2.4 shows a schematic representation of a typical weld metal cooling curve, as was obtained in this research. By constructing tangents at 100°C intervals on the cooling curves obtained, it is possible to obtain the decrease in temperature with time. It should be mentioned that, at the peak temperature, the cooling rate is zero. However, this analysis is being applied at much lower temperatures, when the cooling rates are substantial. Table 2.2 shows how the cooling rate varied as a function of temperature in the four weld deposits. The cooling rate at 1350°C is given for weld 3, when the peak temperature recorded did not reach 1400°C. Sometimes the the curves were not truly smooth but fluctuated making some cooling rates uneven, and the calculated cooling rate correspondingly unreliable. This difficulty is denoted by parentheses.

---

will not appear continuous in these micrographs since they were inserted at an acute angle into the weld. The micrographs are merely intended to show the positions of the thermocouples within the welds. The variation in weld size arises because of the different welding conditions which were used in the four welds. Etchant: swab-etched in aqueous $NH_4S_2O_3$.

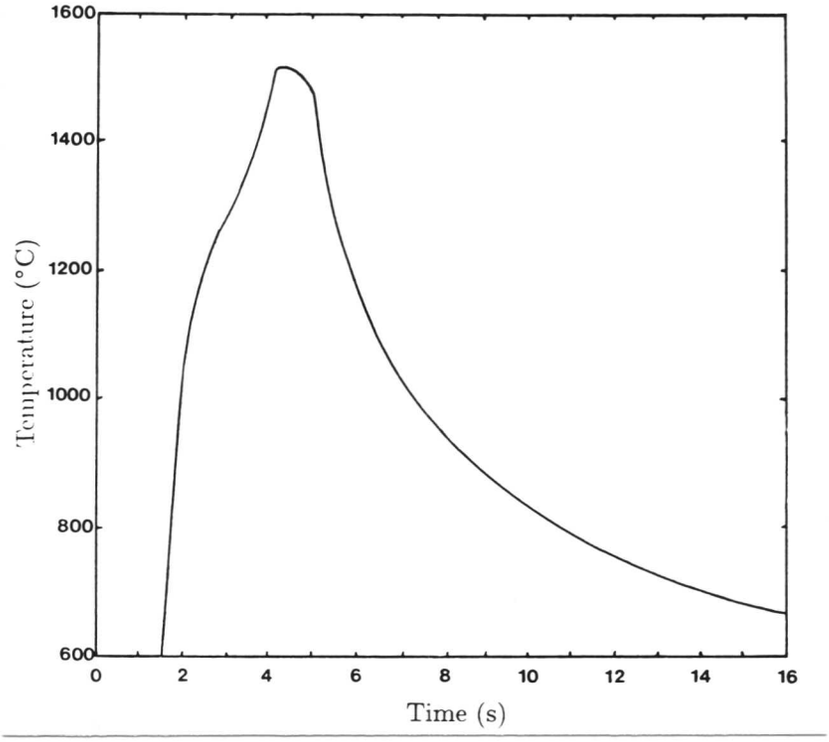

Figure 2.4: Schematic representation of cooling curve for a weld recorded near the solidification temperature. The initial instability prior to the peak temperature arises from the physical displacement of the thermocouple as it is inserted in the weld, exacerbated by the turbulent conditions within the weld pool itself.

T/°C	Weld cooling rate/°C s^{-1}			
	2.1	2.2	2.3	2.4
1000	104	30.3	17.4	-
1100	157	(52.7)	19.2	18.2
1200	244	49.6	36.2	29.0
1300	314	(36.5)	38.6	32.1
1350	-	-	103	-
1400	342	158	-	(32.3)

Table 2.4: Cooling rate as a function of temperature for the four experimental welds.

It can be seen that between welds 2.1 and 2.4, the cooling rates resulting from the different process conditions vary by an order of magnitude. The weld metal was found to have a composition

$$Fe - 0.04C - 1.07Mn - 0.32Si - 0.05Ni - 0.04Cr - 0.1Cu - 0.016P - 0.016S \text{ wt\%}$$

Using a model due to Kirkaldy *et al.* (1978)† the alloy was predicted to have an equilibrium solidus temperature of 1515°C. In fact, this temperature will be depressed, since solidification temperature is a function of cooling rate (Fredriksson, 1976; Jernkontoret, 1977), but the temperature at which freezing was complete could be about 1500°.

Figures 2.5a-d plot the cooling rates experienced by the welds as a function of temperature. The simplest approximation which may be inferred from the experimental data would be that the cooling rate over a given temperature range is proportional to the temperature of the weld. In order to find the best fit lines, the hollow points in Figures 2.5b and d, whose validity was questionable, were given a relative weighting of 0.5. It is thus possible to estimate the cooling rates experienced by the weld at the point of solidification (taken to be 1500°) as follows:

Weld 2.1: 422°C s^{-1}
Weld 2.2: 153°C s^{-1}
Weld 2.3: 104°C s^{-1}
Weld 2.4: 56.5°C s^{-1}

† Discussed in detail in Chapter 4.

a)

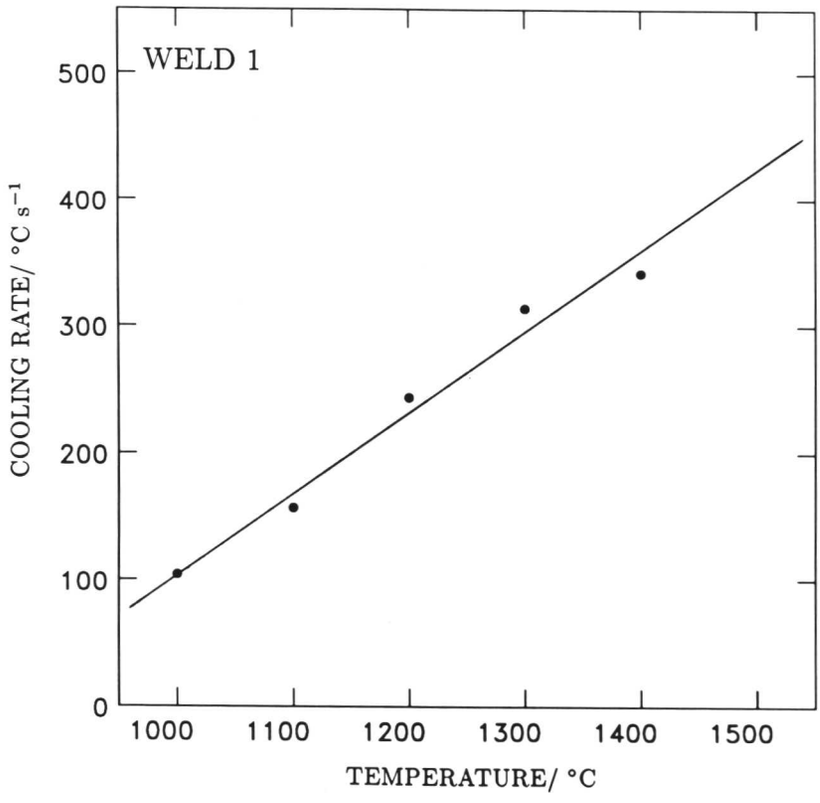
WELD 1
500
400
300
200
100
0
COOLING RATE/ °C s⁻¹
1000
1100
1200
1300
1400
1500
TEMPERATURE/ °C

b)

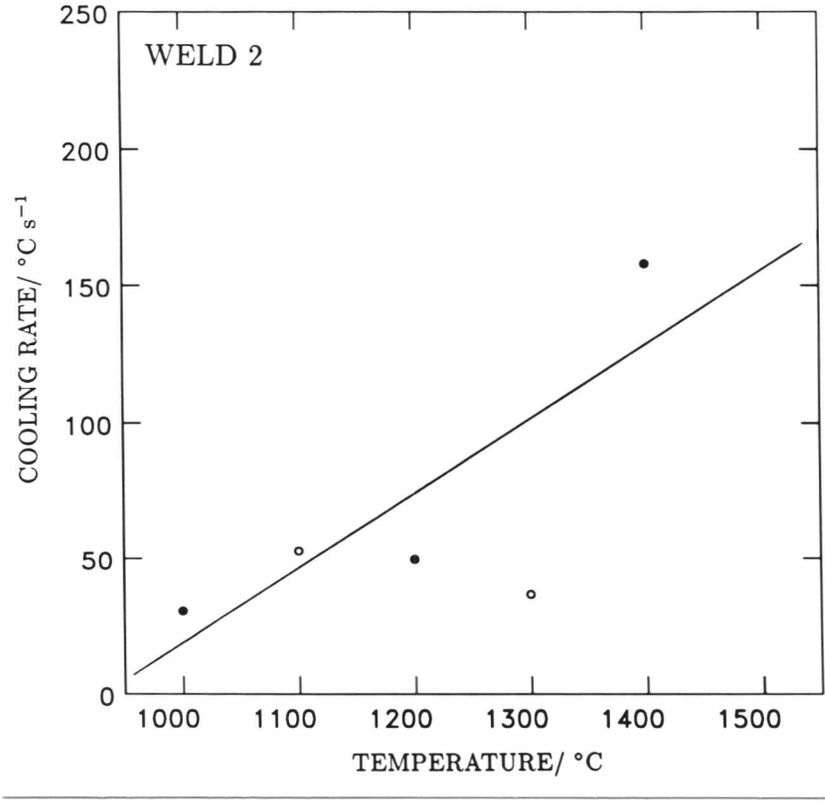
WELD 2
250
200
150
100
50
0
COOLING RATE/ °C s⁻¹
1000
1100
1200
1300
1400
1500
TEMPERATURE/ °C

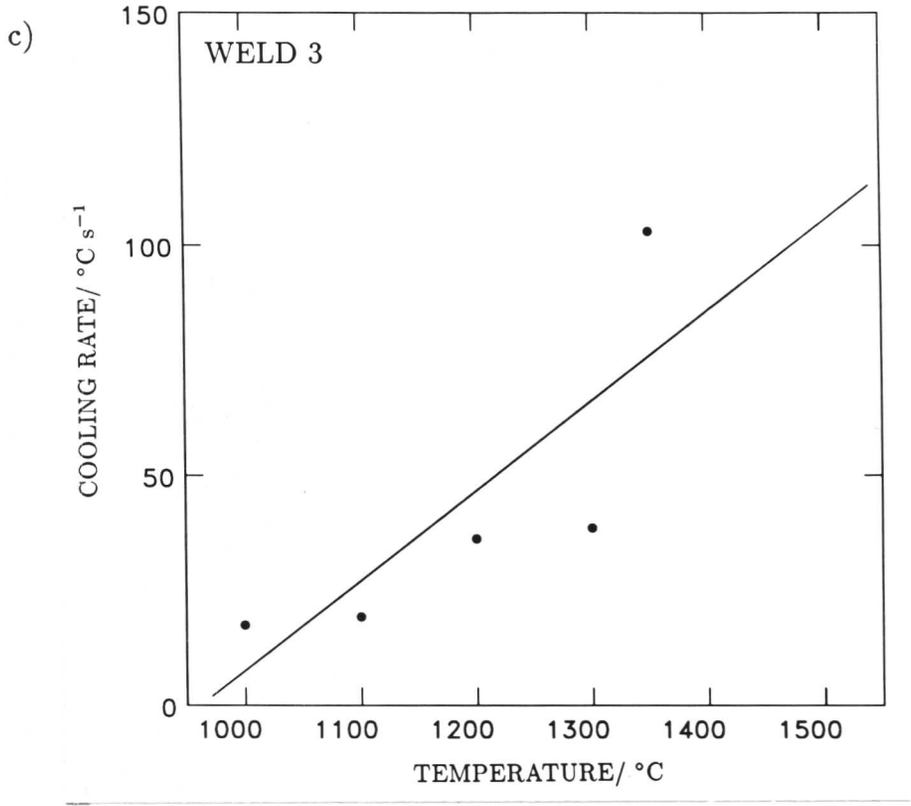

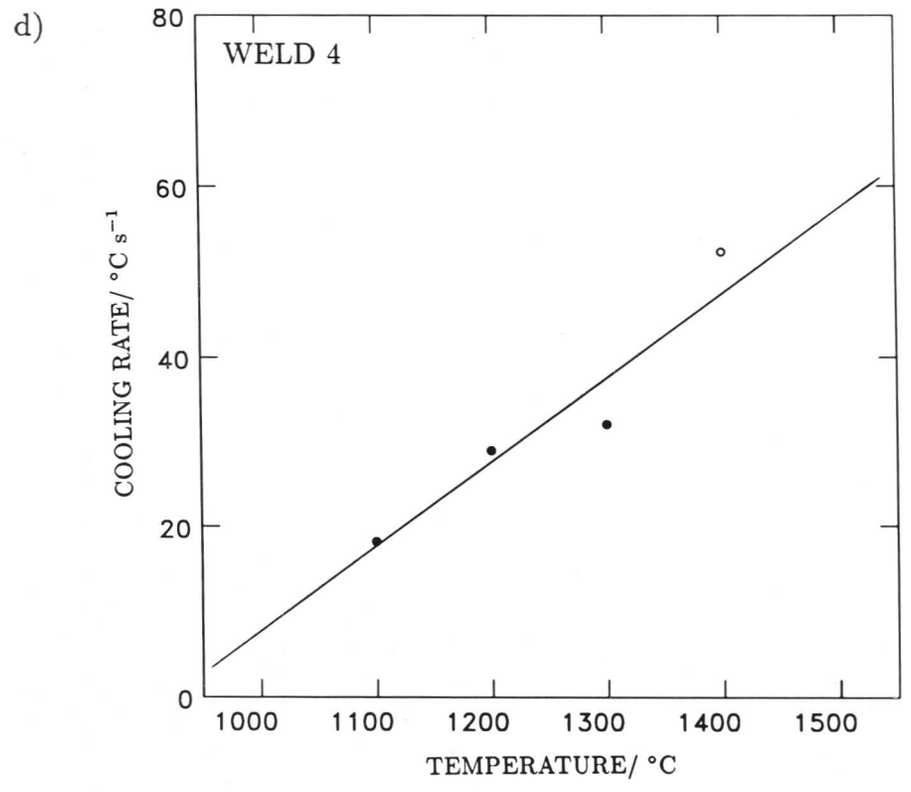

Figures 2.5a-d: Weld metal cooling rates as a function of temperature. (The hollow points are less accurate, and are given a half weighting).

2.4 ANALYSIS OF EXPERIMENTAL RESULTS

Figure 2.6 schematically shows the isotherms around the heat source in fusion welding. The shape of these isotherms can be predicted by considering the temperature distribution in a metal due to a moving point source. For a given heat source, moving at uniform velocity, a quasi-stationary temperature distribution will exist. So, if the arc moves along the x coordinate as shown, the resulting heat distribution in a three dimensional solid plate is given by

$$\frac{d^2T}{dx^2} + \frac{d^2T}{dy^2} + \frac{d^2T}{dz^2} = 2kv\frac{dt}{d(x-vt)} \tag{2.1}$$

where k is the thermal conductivity of the metal being welded

v is the velocity of the arc along the x axis

and t is the thickness of the plate being welded (Rosenthal, 1941; 1946).

The solution to this equation gives the temperature distribution about the moving heat source in the form of isotherms in the solid metal. The distance between isotherms in a given direction, (x, y, z) is approximately given by

$$\lambda(x, y, z) \propto \frac{q}{kvt} \tag{2.2}$$

where q is the heat flux, or rate of heat input.

Subsequent models have attempted to take account of various welding variables, such as surface heat losses (Jhaveri *et al.*, 1962), and the removal of latent heat (Ghent *et al.*, 1979). Nevertheless, despite the various assumptions, Rosenthal's equations have been found to give good agreement for isotherms around the heat source in welding, especially in the welding of thin sheet, when heat flow is largely two-dimensional (American Welding Society, 1976).

Depending upon whether heat flow in the weld can be regarded as three-dimensional downwards as well as lateral, the cooling rate of a weld metal at the centreline may be described by either thick or thin plate equations.

The thick plate equation, which considers three-dimensional heat flow from a point source states that the cooling rate

$$R_{(T)} = \frac{2\pi k}{H_{net}}(T - T_\circ)^2 \tag{2.3}$$

where T is the temperature elevation above $T_\circ$, the initial temperature of the plate

and k is the thermal conductivity.

H_{net} is the weld heat input rate, often referred to simply as the heat input, and is related to the welding parameters thus

$$\begin{aligned} H_{net} &= \frac{q}{v} \\ &= \frac{UI}{v}\eta \end{aligned} \tag{2.4}$$

where U is the welding voltage, equal to 22V

I is the welding current, equal to 180A

and η is the coefficient of arc efficiency, taken as 0.775 for manual-metal-arc welding (Easterling, 1983).

The thin plate equation gives

$$R_{(T)} = 2\pi k\rho C\left(\frac{t}{H_{net}}\right)^2 (T - T_\circ)^3 \tag{2.5}$$

where t is the plate thickness, equal to 12mm

and ρC is the volumetric specific heat, equal to the product of the density of the material being welded, and its specific heat. For low-alloy steel, $\rho = 7.87 \times 10^{-6}$kg

mm^{-3}, and the specific heat of iron at, and close to, its freezing point, $C = 835J$ K^{-1} kg^{-1} (Touloukian and Ho, 1981).

To find which equation is appropriate, (*i.e.* whether thick plate or thin plate conditions prevail), the Adams' "relative plate thickness" criterion is applied. The relative plate thickness is a dimensionless quantity defined as (American Welding Society, 1976).

$$\tau = t\sqrt{\frac{\rho C(T - T_o)}{H_{net}}} \tag{2.6}$$

The thick plate equation applies when τ is greater than 0.9, and the thin plate equation when τ is less than 0.6. Values for the relative plate thicknesses of the four welds are given in Table 2.5 for $T = 1500°C$.

Weld	τ
2.1	1.03
2.2	0.80
2.3	0.62
2.4	0.62

Table 2.5: Relative plate thicknesses for Welds 1-4.

Therefore, from the values obtained, for Weld 2.1, the thick plate equation applies. For welds 2.2, 2.3 and 2.4, the thick plate equation should give a cooling rate which is too high, and the thin plate equation, one which is too low. $k_{(\delta-\mathrm{Fe}/1811K)}$ has been taken as $0.039 WK^{-1}mm^{-1}$ (Touloukian and Ho, 1981)

Theoretical and measured values for the cooling rates of the four welds at 1495°C are given in Table 2.6, and are plotted against one another in Figure 2.7.

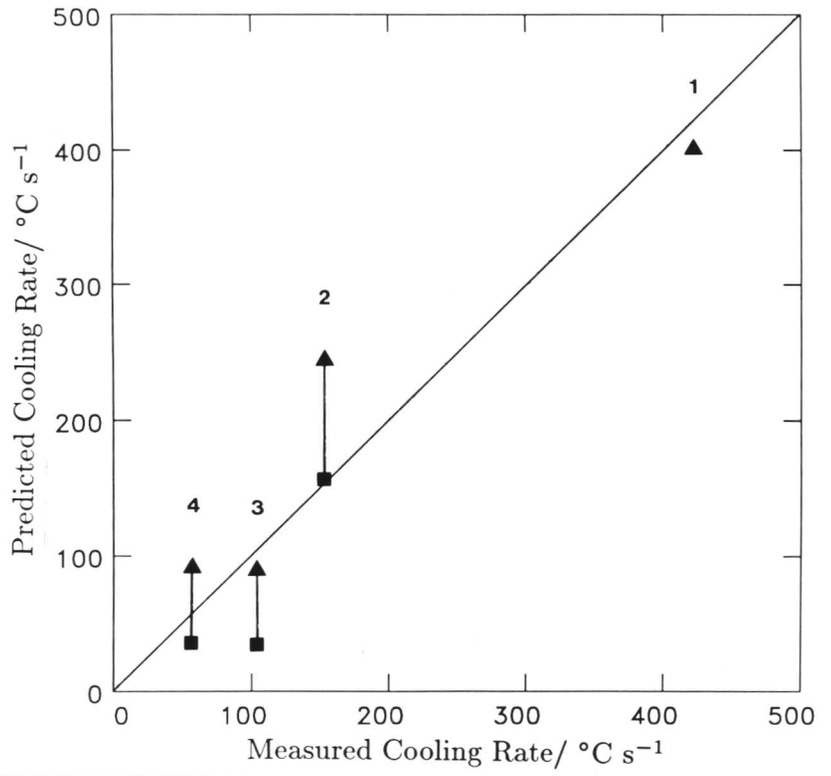

Figure 2.7: Measured cooling rates for welds 1-4, compared against thick plate (▲) and thin plate (■) predictions. (For Weld 1, the thin plate equation was not applicable).

Cooling Rate/°C	Weld			
	2.1	2.2	2.3	2.4
Measured	422	153	104	56.5
Thick plate	401	244	88.5	90.5
Thin plate	–	156	34.2	35.3

Table 2.6: Measured and calculated cooling rates at 1500°C

The experimental results provide quantitative data on the cooling rates encountered in weld deposits. The agreement of heat flow calculations with the experimental weld cooling rates is, in fact, better than expected, since the equations were not specifically developed from or for high temperature measurements. Also, the equations take no account of the finite size of the heat source, or of convection within the weld pool, and were not developed from high temperature measurements.

It is instructive to compare these results with those of Edvardsson (1975), who found in controlled directional solidification experiments, that an Fe-0.19C-1.47Mn-0.42Si wt% steel, cooled at 33°C/s, solidified as primary austenite. These results differ to those obtained in Weld 2.1, and suggest, therefore, that results obtained from directional solidification cannot readily be used to model weld pool solidification, perhaps because the influence of the base-plate on the solidification mode in welding needs to be taken into account.

2.5 SUMMARY

Solidification processes during manual-metal-arc welding have been studied, and observed changes in primary microstructure have been related to chemical composition and cooling conditions.

A cooling rate of approximately 600°C/s at the solidus temperature, estimated using empirical heat flow equations was found to result in solidification as δ-ferrite in a 0.19wt% C low-alloy C-Mn weld deposit, but to induce solidification in a 0.31 wt% C weld. This is a consequence of the high cooling rates which cause primary austenite precipitation, when under equilibrium conditions, δ-ferrite would be expected. The cooling rates experienced by manual-metal-arc welds at the point of solidification have been estimated for varying travel speeds and preheats.

A method is described for measuring the cooling rates at, and near to, the solidification temperature of the weld pool by injecting a shielded thermocouple into the weld pool subsequent to the passage of the arc. Preinsertion of thermocouples was tried as a means by which the cooling rates during weld metal solidification could be measured. Unfortunately, conditions under the arc are so severe that the thermocouples there did not survive, and it is concluded that direct pre-insertion is not a viable means by which to measure $\left(\frac{dT}{dt}\right)$ in a weld. That is not to say, however, that such a technique might not be practicable if modified.

Harpooning of the weld was more successful, with the temperature sensor being frozen into the weld pool during solidification. For a typical welding speed (2.3mm/s) the cooling rate in manual-metal-arc welding was found to be high, at over 400°C/s in the early stages of freezing. However, a reduction in travel speed and application of preheat have been found to reduce the rate of cooling substantially. Initial calculations show that measured cooling rates agreed with empirical thin-plate and thick-plate equations.

This work provides a preliminary basis for the quantitative prediction of the cooling rates experienced by welds during solidification.

REFERENCES

AMERICAN WELDING SOCIETY (1976), "Welding Handbook", Ed., Charlotte Weisman, 7th Ed., American Welding Society, Miami, Fla. 33215, **1**, 84-88.

BAKER, R. G. (1976), "Rosenhain Centenary Conference", *[Proc. Conf.]*, The Royal Society, London, U.K., 207-223.

BARLOW, J. A. (1982), *Weld. Inst. Res. Bull.*, Welding Institute, Abington, U.K., (1), 5-8.

BHADESHIA, H. K. D. H., SVENSSON, L-E., and GRETOFT, B., (1985) *Acta Metall.*, **33**, 1271-1283.

DAVIES, G. J. and GARLAND, J. G. (1975), *Int. Met. Rev.*, **20**, No. 196, 83-106.

EASTERLING, K. E., (1983) "Introduction to the Physical Metallurgy of Welding", Butterworths, London.

EDVARDSSON, T. (1975), Ph.D. thesis, Swedish Institute for Metals Research, Stockholm, Sweden.

FREDRIKSSON, H. (1976), *Met. Sci.*, (3), 77-86.

FREDRIKSSON, H. and STJERNDAHL, J. (1982), *Ibid.*, **16**, (10), 575–585.

GARLAND, J. G. and KIRKWOOD, P. R. (1974), IIW Doc. IX-892-74.

GHENT, H., HERMANCE, C. E., KERR, H. W., and STRONG, A. N. (1979), "Arc Physics and Weld Pool Behaviour", *[Proc. Conf.]*, Welding Institute, Abington, U.K., paper 3.

JHAVERI, P., MOFFATT, W. G., and ADAMS, C. M. (1962), *Weld. J.*, **41**, Res. Supp., 12s-16s.

JERNKONTORET, (1977), "A Guide to the Solidification of Steels", Jernkontoret, Box 1721, S11187 Stockholm, Sweden, Section 1.

KIRKALDY, J. S., THOMSON, B. A., and BAGANIS, E. A. (1978), "Hardenability Concepts with Applications to Steels", *[Proc. Conf.]*, Eds., D. V. Doane and J. S. Kirkaldy, *Met. Soc. AIME*, AIMMPE, Warrendale, PA15086, U.S.A., 82-125.

KOHNO, R. and JONES, S. B. (1978), *Weld. Inst. Res. Rep.*, Welding Institute, Abington, U.K., 81/1978/PE.

PORTER, D. A. and EASTERLING, K. E. (1981), "Phase Transformations in Metals and Alloys, Van Nostrand Reinhold, U.K.

RASANEN, E. and TEKULA, J. (1972), *Scand. J. Metall.*, **1**, 75-80.

ROSENTHAL, D. (1941), *Weld. J.*, **20**, Weld. Res. Supp., 220s-234s.

ROSENTHAL, D. (1946), *Trans. AIME*, **68**, 849-866.

SVENSSON, L-E., BHADESHIA, H. K. D. H., and GRETOFT, B., (1986) *Scand. J. Metall.*, **15**, 97-103.

TOULOUKIAN, Y. S. and HO, C. Y., (1981) "Properties of Selected Ferrous Alloying Elements", McGraw-Hill, New York, 100–104.